The Effects of Exfoliation, Organic Solvents and Anodic Activation on Catalytic Hydrogen Evolution Reaction of Tungsten Disulfide

Electronic Supplementary Material (ESI) for Nanoscale.

Supporting Information

The Effects of Exfoliation, Organic Solvents and Anodic Activation on Catalytic Hydrogen Evolution Reaction of Tungsten Disulfide

Wanglian Liu,[a, b] John Benson,[c] Craig Dawson,[c] Andrew Strudwick,[c] Arun Prakash Aranga Raju,[c] Yisong Han, [a] Meixian Li,*[, b] and Pagona Papakonstantinou*[, a]

[a] School of Engineering, Engineering Research Institute, Ulster University, Newtownabbey BT37 0QB, United Kingdom.

[b] College of Chemistry and Molecular Engineering, Peking University, Beijing 100871, People's Republic of China.

[c] 2-DTech Ltd, Core Technology Facility, 46 Grafton St, Manchester M13 9NT, United Kingdom.

*Corresponding authors' e- mails: lmwx@pku.edu.cn; p.ppakonstantinou@ulster.ac.uk

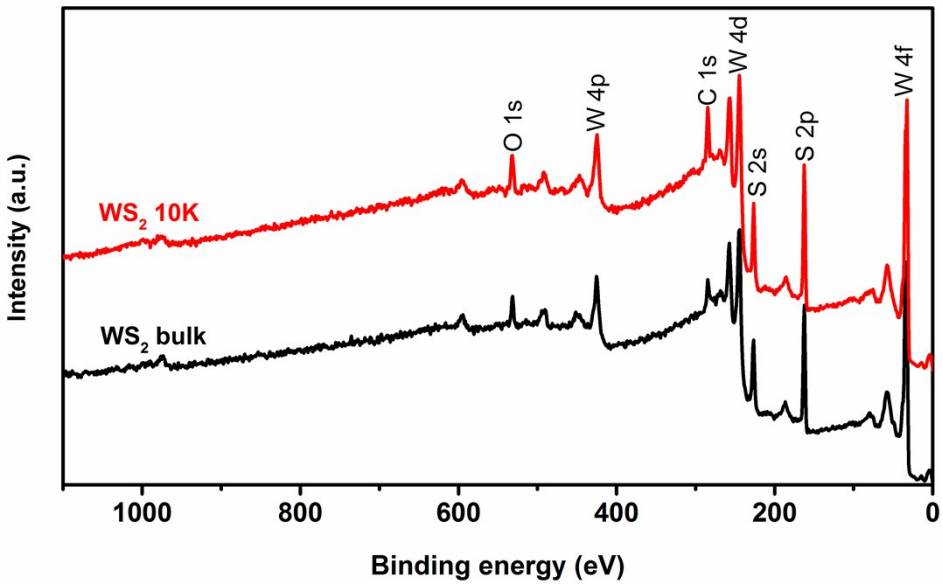

Fig. S1 XPS surveys of WS_2 bulk and WS_2 10K.

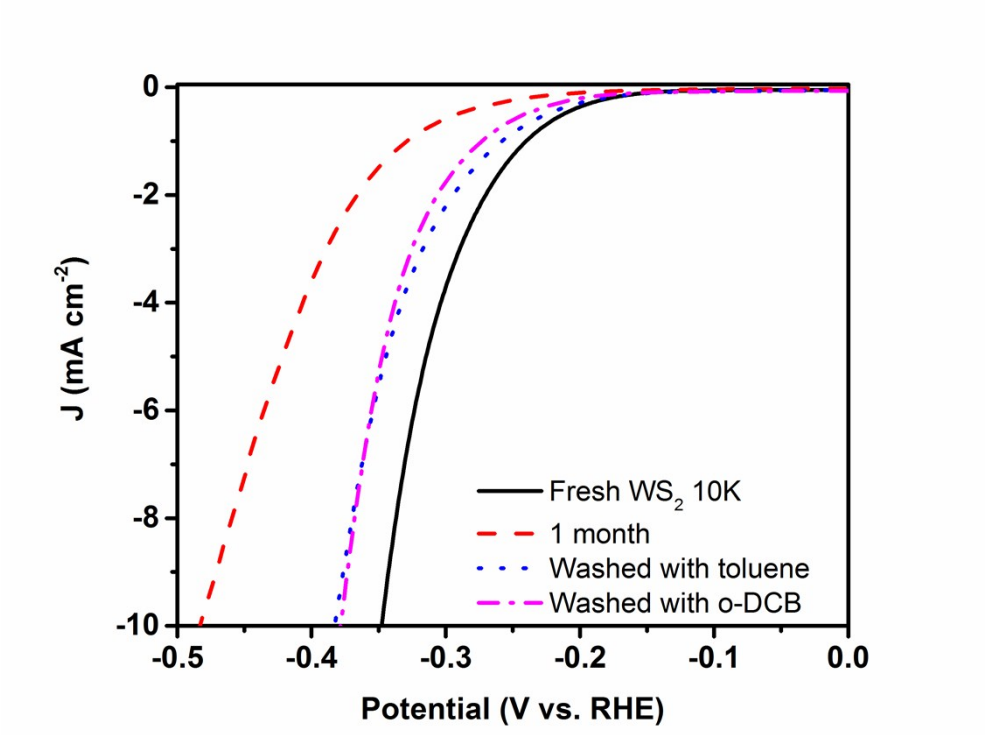

Fig. S2 Polarization curves of electrodes modified with i) freshly prepared WS_2 10K dispersion; ii) WS_2 10K dispersion 1 month old (1 month); iii) WS_2 10K dispersion 1 month old, washed with toluene and iv) WS_2 10K dispersion 1 month old, washed with o-dichlorobenzene (o-DCB).

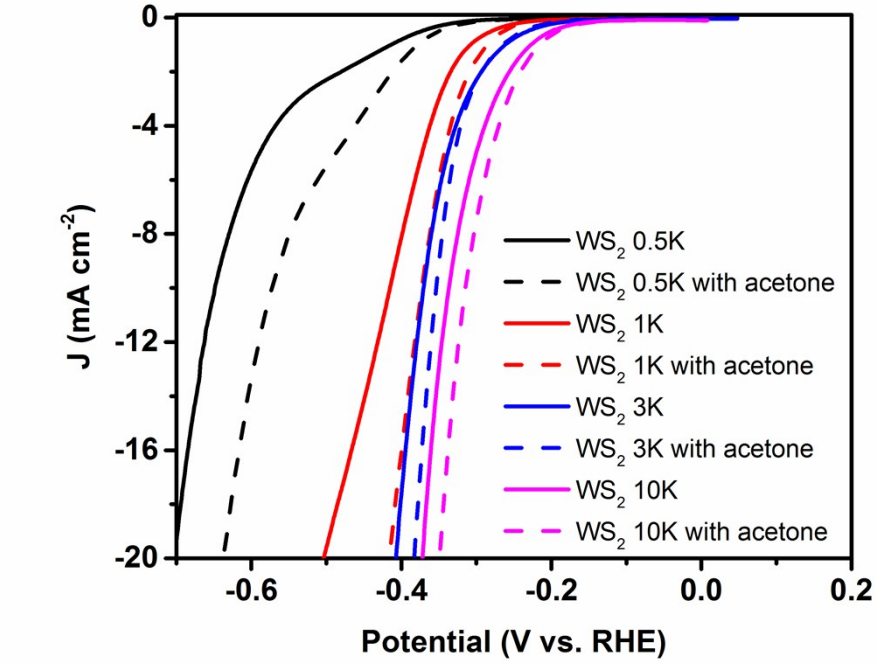

Fig. S3 Polarization curves of the electrodes modified with fresh 0.5K, 1K, 3K and 10K dispersions before (full lines) and after (dashed lines) washing with acetone.

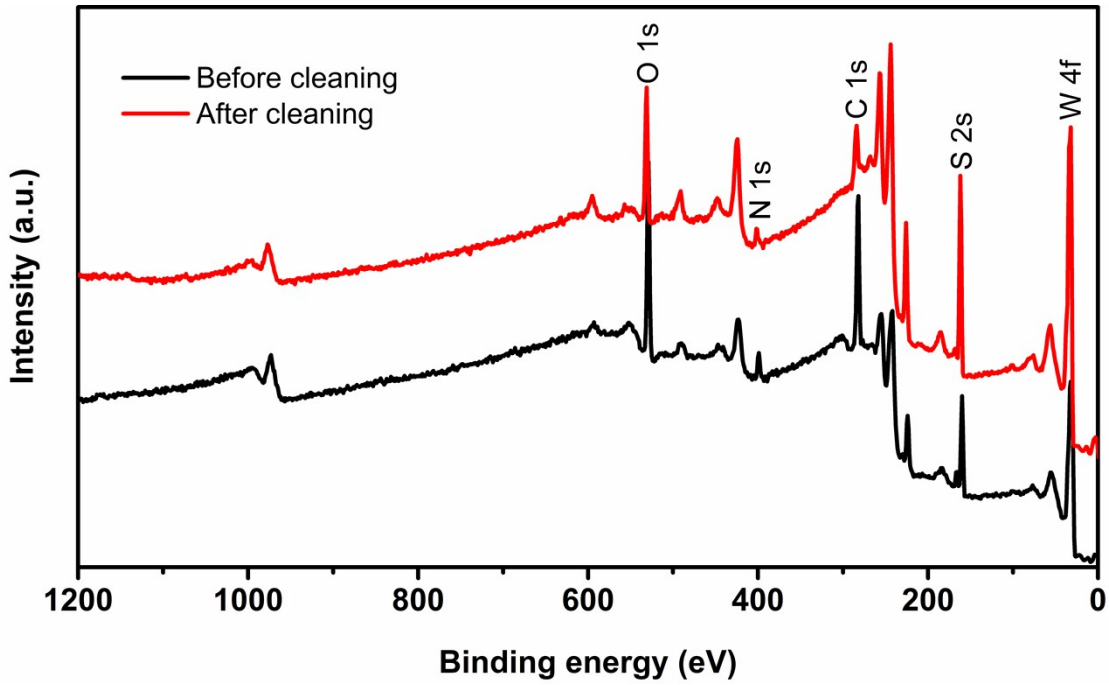

Fig. S4 XPS surveys of a GCE electrode modified with 1 month old WS_2 10K dispersion before and after cleaning with acetone.

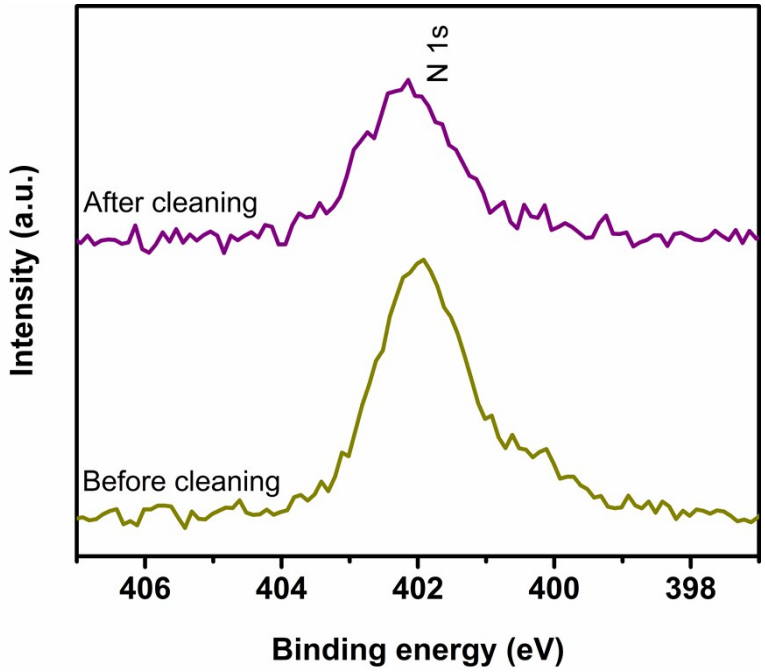

Fig. S5 High-resolution N1s core level XPS spectra from a GCE electrode modified with 1 month old WS_2 10K dispersion before and after cleaning in acetone.

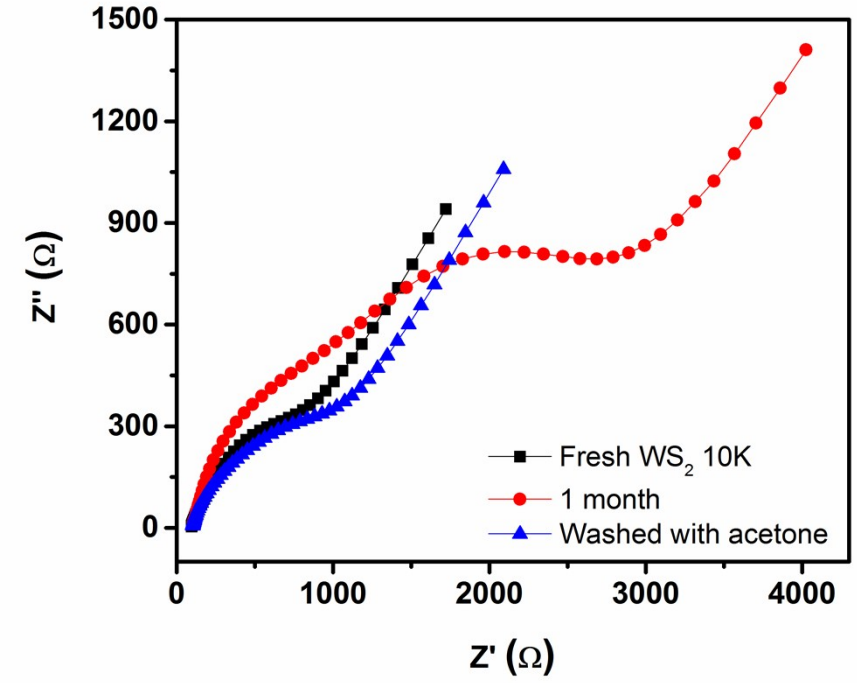

Fig. S6 Electrochemical impedance spectra of the electrodes modified with i) freshly prepared WS_2 10K dispersion; ii) WS_2 10K dispersion 1 month old and iii) WS_2 10K dispersion 1 month old, washed with acetone. The measurements were conducted in 0.1 M KCl-0.01 M phosphate buffer solution (pH = 7.4) containing 5 mM $K_3Fe(CN)_6$-$K_4Fe(CN)_6$ (1:1).

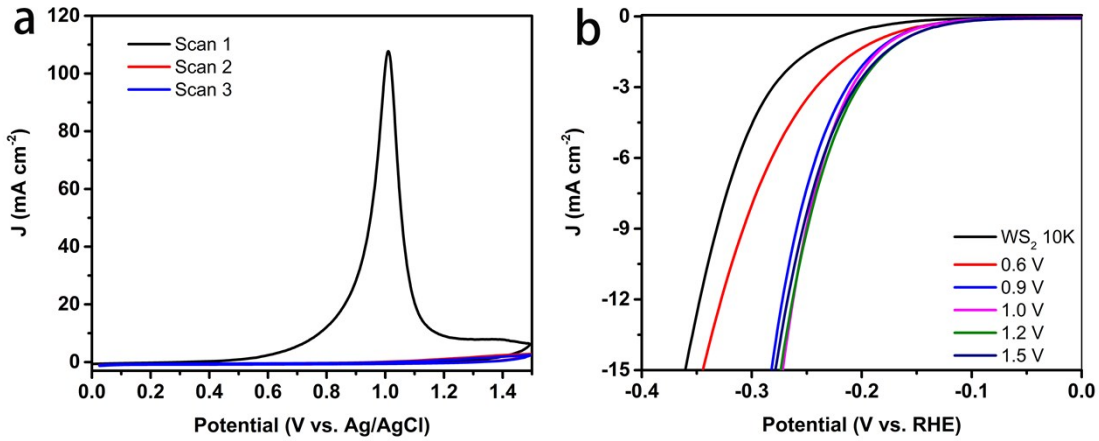

Fig. S7 a) Cyclic voltammetry scans of a WS_2 10K modified electrode performed between 0 and 1.5 V (vs. Ag/AgCl) in 0.5 M H_2SO_4. b) Polarization curves of WS_2 10K modified electrodes before and after activation at different potentials in 0.5 M H_2SO_4.

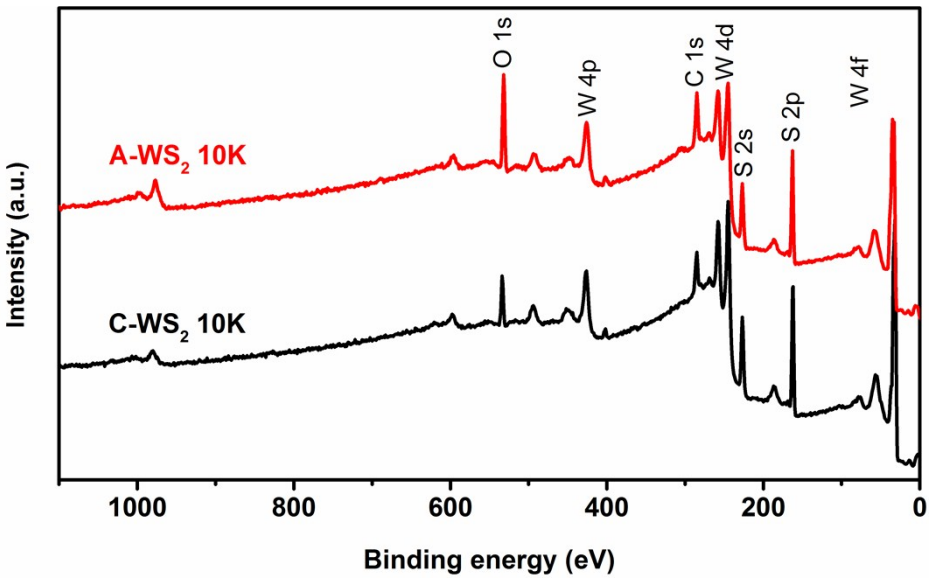

Fig. S8 XPS surveys of WS_2 10K before (C-WS_2 10K) and after (A-WS_2 10K) activation.

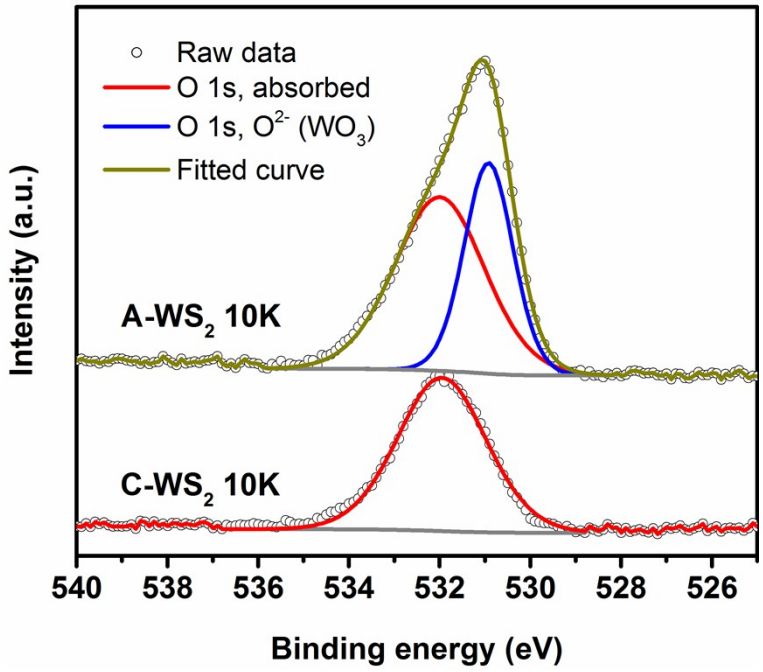

Fig. S9 High resolution O 1s core level XPS spectra of WS_2 10K before (C-WS_2 10K) and after (A-WS_2 10K) activation.

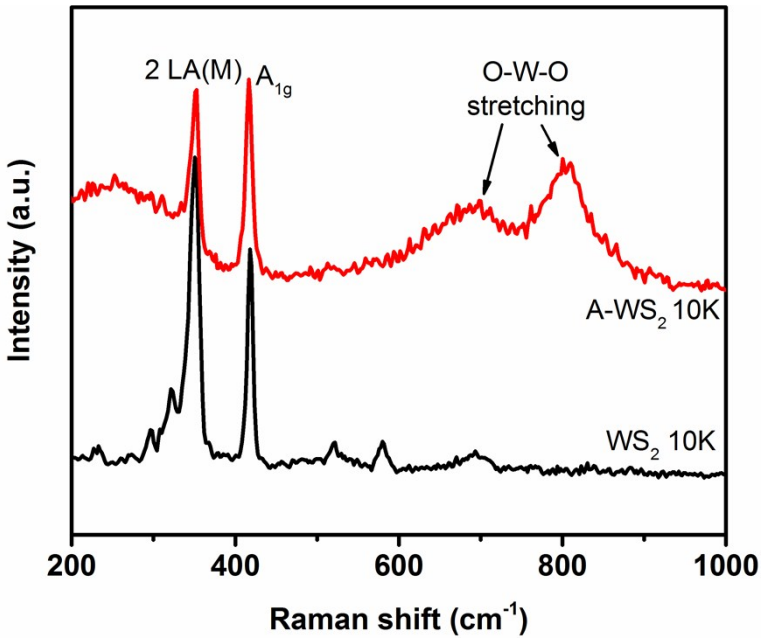

Fig. S10 Raman spectra of WS_2 10K before (WS_2 10K) and after (A-WS_2 10K) activation.

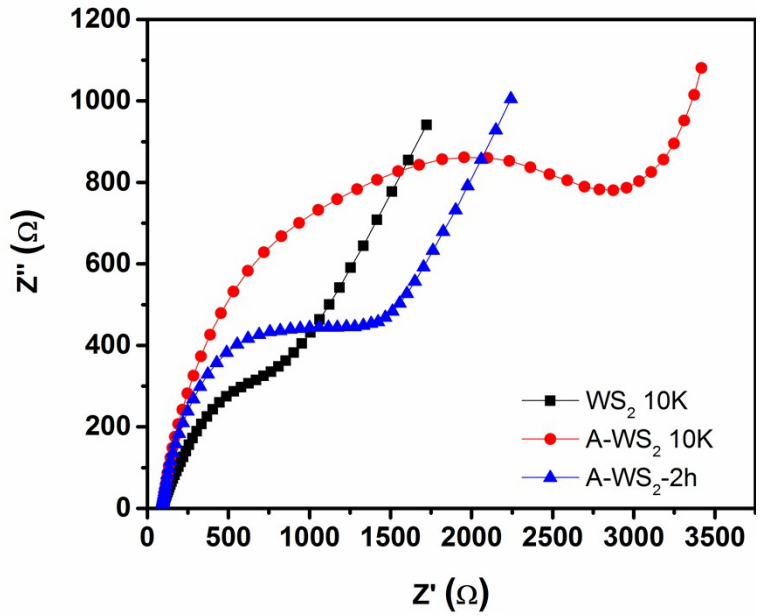

Fig. S11 Electrochemical impedance spectra of a WS_2 10K electrode: i) before activation (WS_2 10K); ii) after activation (A-WS_2 10K) and iii) after activation and 2 hours HER test (A-WS_2-2h). EIS was conducted in 0.1 M KCl-0.01 M phosphate buffer solution (pH = 7.4) containing 5 mM $K_3Fe(CN)_6$-$K_4Fe(CN)_6$ (1:1).

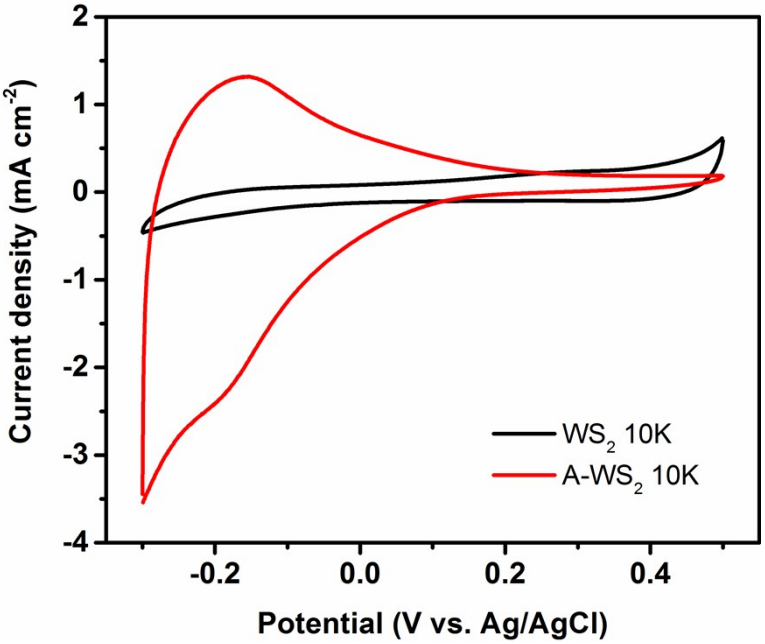

Fig. S12 Cyclic voltammograms performed between 0.5 and -0.3V (vs. Ag/AgCl) with a scan rate of 100 mV s^{-1} in 0.5 M H_2SO_4 for i) WS_2 10K and ii) activated WS_2 10K (A-WS_2 10K), respectively.

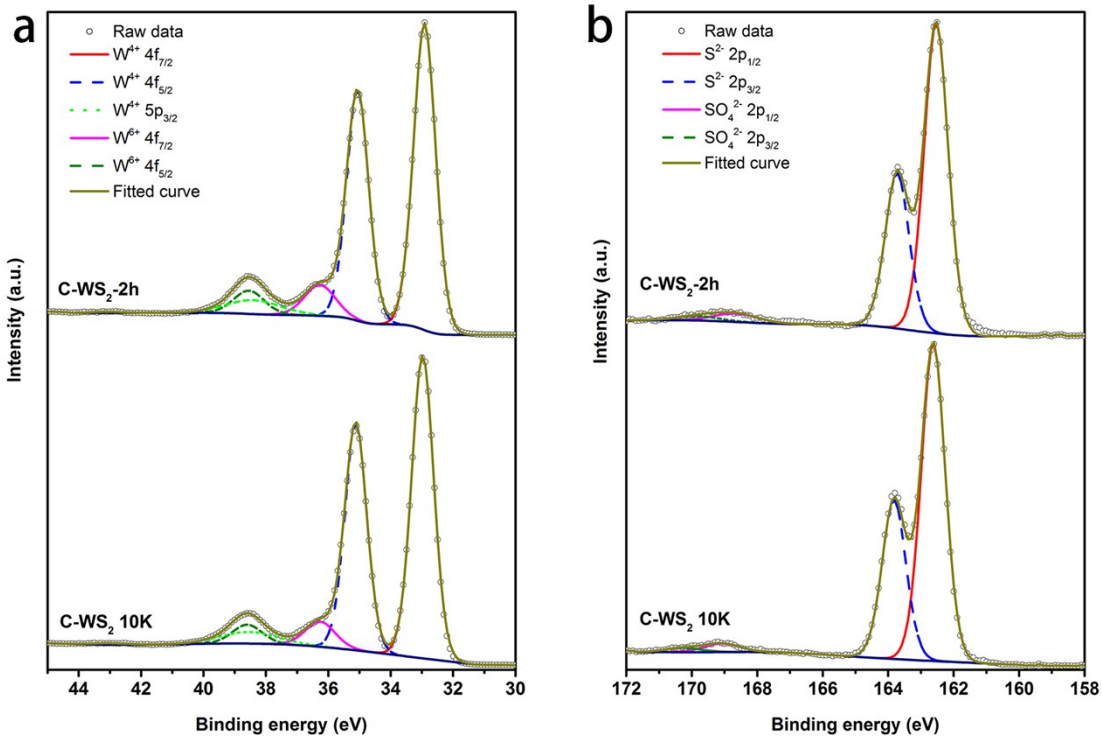

Fig. S13 High resolution (a) W 4f and 5p and (b) S 2p core level XPS spectra of controlled WS_2 10K before (C-WS_2 10K) and after (C-WS_2-2h) 2h HER test.

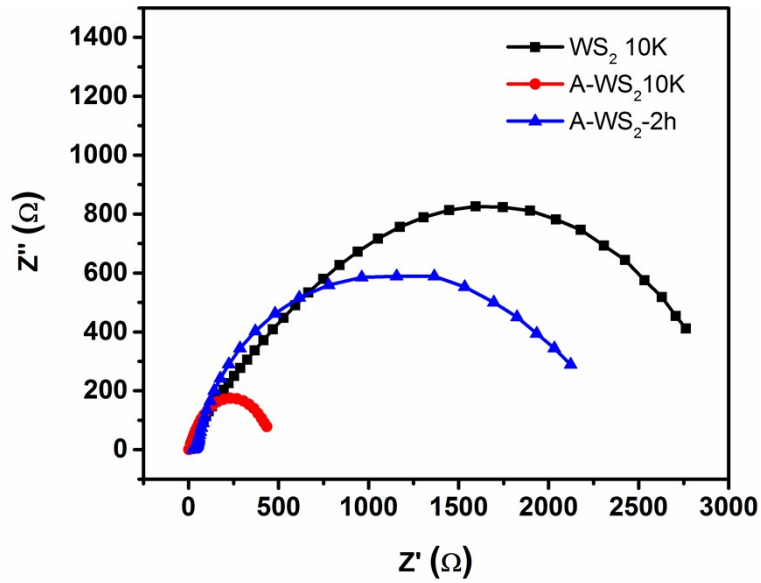

Fig. S14 Electrochemical impedance spectra of i) WS_2 10K; ii) activated WS_2 10K (A-WS_2 10K) and iii) activated WS_2 10K subjected to 2 hours HER test (A-WS_2-2h) in 0.5 M H_2SO_4.

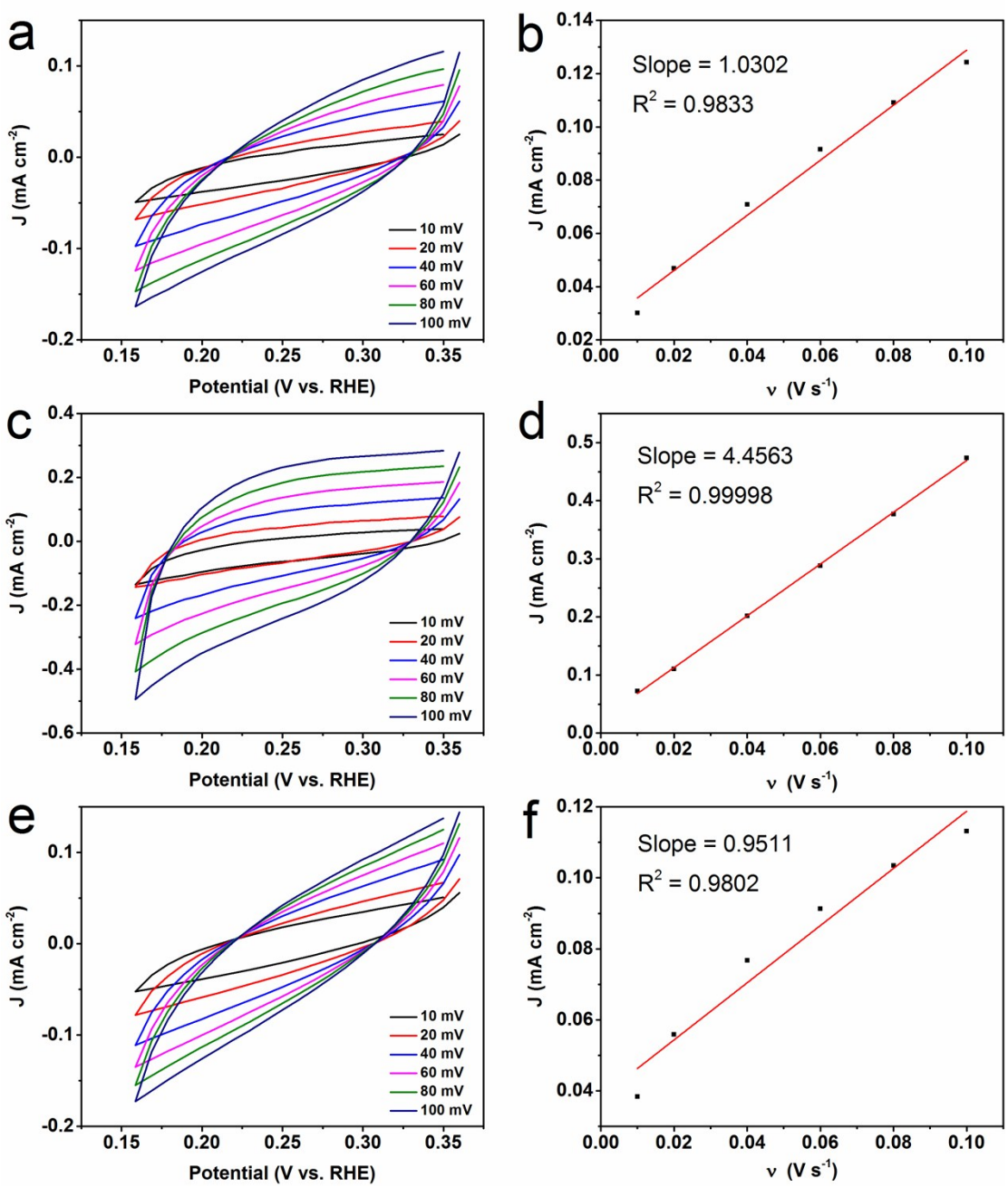

Fig. S15. Cyclic voltammogram scans of (a) WS_2 10K, (c) a-WS_2 10K and (e) a-WS_2-2h at different scan rates (0.1, 0.08, 0.06, 0.04, 0.02 and 0.01 V s^{-1}) and the corresponding capacitive current density measured at 0.25 V (vs. RHE) plotted as a function of scan rate (b, d, f). The average value of the slope was determined as the double-layer capacitance (C_{dl}) of each catalyst. The calculated C_{dl} of WS_2 10K, A-WS_2 10K and A-WS_2-2h are 1.03, 4.46 and 0.95 mF cm^{-2}, respectively.

Table S1 XPS data of composition of WS_2 bulk and 500, 1K, 3K and 10K centrifugation products.

	WS_2 bulk	WS_2 0.5K	WS_2 1K	WS_2 3K	WS_2 10K

S (%At conc)	65.5	65.2	65.2	65.4	66.0
W (%At conc)	34.5	34.1	34.8	34.6	34.0
Ratio of S to W	1.9 : 1	1.9 : 1	1.9 : 1	1.9 : 1	1.9 : 1

Table S2 The atomic ratios of S to W and W(VI) to W(IV) of controlled WS_2 10K (C-WS_2 10K), activated WS_2 10K (A-WS_2 10K), activated WS_2 10K subjected to 0.5 and 2 hours HER test (A-WS_2-0.5h and A-WS_2-2h) and controlled WS_2 10K subjected to 2 hours HER test (C-WS_2-2h).

	C-WS_2 10K	A-WS_2 10K	A-WS_2-0.5h	A-WS_2-2h	C-WS_2-2h
Ratio of S to W	1.9 : 1	1.6 : 1	1.7 : 1	1.8 : 1	1.9 : 1
Ratio of W(VI) to W(IV)	0.1 : 1	0.4 : 1	0.3 : 1	0.2 : 1	0.1 : 1

Table S3 Comparison of the electrocatalytic activity of WS_2 nanosheets/nanodots (WS_2 NSDs) and activated WS_2 NSDs *versus* the WS_2-based catalysts on GCE (two catalysts on carbon fiber paper and carbon cloth have been pointed out) reported recently for HER in 0.5 M H_2SO_4 .

Catalysts	Mass loading (mg cm^{-2})	Overpotential (mV) for j=10 mA cm^{-2}	Tafel Slope ($mV\ dec^{-1}$)	Reference
WS_2 NSDs	0.283	337	80	This work
Activated WS_2 NSDs	0.283	255	73	This work
WS_2 nanoflakes	1	~358	~200	1
BuLi exfoliated WS_2 nanosheets (~80% 1T- WS_2)	0.001-0.0065	240 (1T) 440 (2H)	55(1T) 110(2H)	2
BuLi exfoliated WS_2	0.0707	~690	~110	3
$WS_{2(1-x)}Se_{2x}$ nanotubes on CFP	0.21	~270	105	4
WS_2 on carbon cloth	-	225	105	5
WS_2 nanosheets	0.0566	~380	~95	6
WS_2 nanosheets/quantum dots	0.0354	~340 (DMF)	70 (DMF)	7

		~355 (NMP)	75 (NMP)	
Aromatic-exfoliated WS_2	0.0142	~520	~70	8
WS_{3-x} Films	-	494	43.7	9
Ta-doped WS_2	0.0707	~720	~170	10

1. Choi, C. L.; Feng, J.; Li, Y.; Wu, J.; Zak, A.; Tenne, R.; Dai, H., WS_2 nanoflakes from nanotubes for electrocatalysis. *Nano Res.* **2013**, *6,* 921-928.

2. Voiry, D.; Yamaguchi, H.; Li, J.; Silva, R.; Alves, D. C.; Fujita, T.; Chen, M.; Asefa, T.; Shenoy, V. B.; Eda, G.; Chhowalla, M., Enhanced catalytic activity in strained chemically exfoliated WS_2 nanosheets for hydrogen evolution. *Nat. Mater.* **2013**, *12*, 850-855.

3. Eng, A. Y. S.; Ambrosi, A.; Sofer, Z.; Simek, P.; Pumera, M., Electrochemistry of Transition Metal Dichalcogenides: Strong Dependence on the Metal-to-Chalcogen Composition and Exfoliation Method. *ACS Nano* **2014**, *8*, 12185-12198.

4. Xu, K.; Wang, F.; Wang, Z.; Zhan, X.; Wang, Q.; Cheng, Z.; Safdar, M.; He, J., Component-Controllable $WS_{2(1-x)}Se_{2x}$ Nanotubes for Efficient Hydrogen Evolution Reaction. *ACS Nano* **2014**, *8*, 8468-8476.

5. Yan, Y.; Xia, B.; Li, N.; Xu, Z.; Fisher, A.; Wang, X., Vertically oriented MoS_2 and WS_2 nanosheets directly grown on carbon cloth as efficient and stable 3-dimensional hydrogen-evolving cathodes. *J. Mater. Chem. A* **2015**, *3*, 131-135.

6. Chia, X.; Ambrosi, A.; Sofer, Z.; Luxa, J.; Pumera, M., Catalytic and Charge Transfer Properties of Transition Metal Dichalcogenides Arising from Electrochemical Pretreatment. *ACS Nano* **2015**, *9*, 5164-5179.

7. Xu, S.; Li, D.; Wu, P., One-Pot, Facile, and Versatile Synthesis of Monolayer MoS_2/WS_2 Quantum Dots as Bioimaging Probes and Efficient Electrocatalysts for Hydrogen Evolution Reaction. *Adv. Funct. Mater.* **2015**, *25*, 1127-1136.

8. Tan, S. M.; Sofer, Z.; Luxa, J.; Pumera, M., Aromatic-Exfoliated Transition Metal Dichalcogenides: Implications for Inherent Electrochemistry and Hydrogen Evolution. *ACS Catal.* **2016**, *6*, 4594-4607.

9. Tan, S. M.; Pumera, M., Bottom-up Electrosynthesis of Highly Active Tungsten Sulfide (WS_{3-x})

Films for Hydrogen Evolution. *ACS Appl. Mater. Interfaces* **2016**, *8*, 3948-3957.

10. Chua, X. J.; Luxa, J.; Eng, A. Y. S.; Tan, S. M.; Sofer, Z.; Pumera, M., Negative Electrocatalytic Effects of p-Doping Niobium and Tantalum on MoS_2 and WS_2 for the Hydrogen Evolution Reaction and Oxygen Reduction Reaction. *ACS Catal.* **2016**, *6*, 5724-5734.

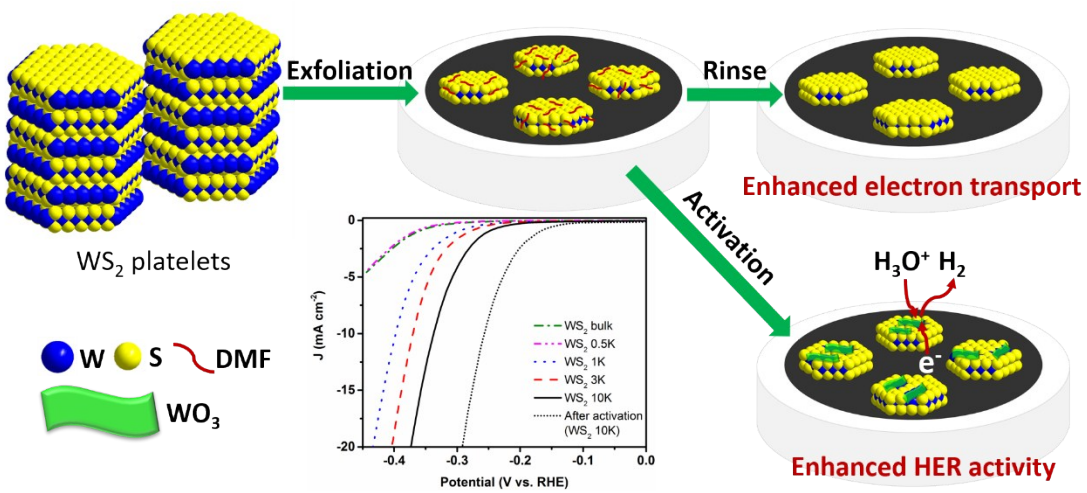
Exfoliation
Rinse
Enhanced electron transport
Activation
WS2 platelets
W
S
DMF
WO3
J (mA cm-2)
Potential (V vs. RHE)
WS2 bulk
WS2 0.5K
WS2 1K
WS2 3K
WS2 10K
After activation (WS2 10K)
H3O+ H2
e-
Enhanced HER activity